Analysis of Human Perception Models for Motion Sickness in Autonomous Driving

Ilhan Yunus [1,2], Fikri Farhan Witjaksono[1,3], Elif Naz Basokur [1,4], Jenny Jerrelind [2], Lars Drugge [2]

[1] *Volvo Car Corporation, SE-405 31 Gothenburg, Sweden*

[2] *The Centre for ECO^2 Vehicle Design, Engineering Mechanics, KTH Royal Institute of Technology SE-100 44 Stockholm, Sweden*

[3] *Department of Mechanical and Maritime Sciences (M2), Chalmers University of Technology, SE-412 96 Gothenburg, Sweden*

[4] *Dept. of Electrical Engineering and Information Technology, ETH Zürich 8092 Zürich, Switzerland*

Presenter: Ilhan Yunus

ilhan.yunus@volvocars.com

Motion Sickness Modelling Overview

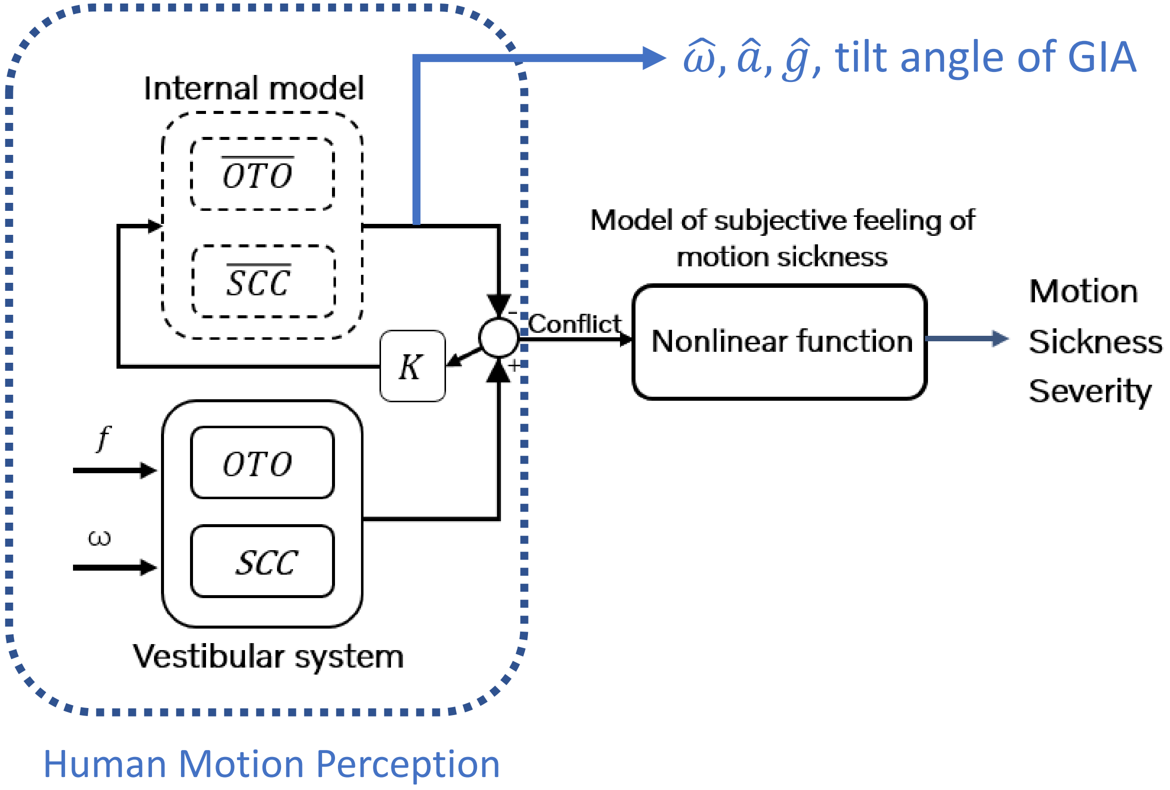

VOLVO

Vestibular Organ Models

Vestibular system

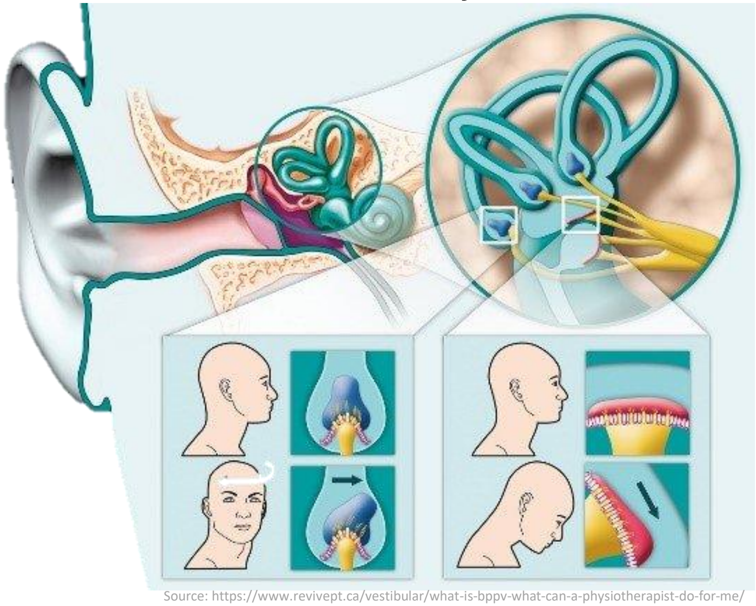

Source: https://www.revivept.ca/vestibular/what-is-bppv-what-can-a-physiotherapist-do-for-me/

Semicircular canals (SCC) detect angular motion

$$H_{SCC} = \frac{\omega_s}{\omega} = \frac{\tau_d \tau_a s^2}{(\tau_d s + 1)\,(\tau_a s + 1)}$$

Otolith (OTO) detect GIF (gravito-intertial force)

$$\boldsymbol{f} = \boldsymbol{g} + \boldsymbol{a}$$

$$H_{OTO} = \frac{f_s}{f} = \frac{\tau_c s + 1}{(\tau_L s + 1)\,(\tau_S s + 1)}$$

Currently Available Models

Modelling Framework	Authors
Luenberger Observer	Haslwanter et. al. (2000), Merfeld (1995, 2002), Vingerhoets et. al. (2007), Newman (2009)
Kalman Filter	Borah (1979) and Lim et. al. (2017)
Extended Kalman Filter (EKF)	Pommellet (1990)
Unscented Kalman Filter (UKF)	Selva (2009)
Particle Filter	Karmali and Merfeld (2012)

Motion Sickness Modeling Framework	Authors
Luenberger Observer	Bos and Bles (1998, 2002), Braccesi and Cianetti (2011), Kamiji et al. (2007), Wada (2015, 2020, 2021,2022)

Human perception models

Merfeld Model (1995, 2001)

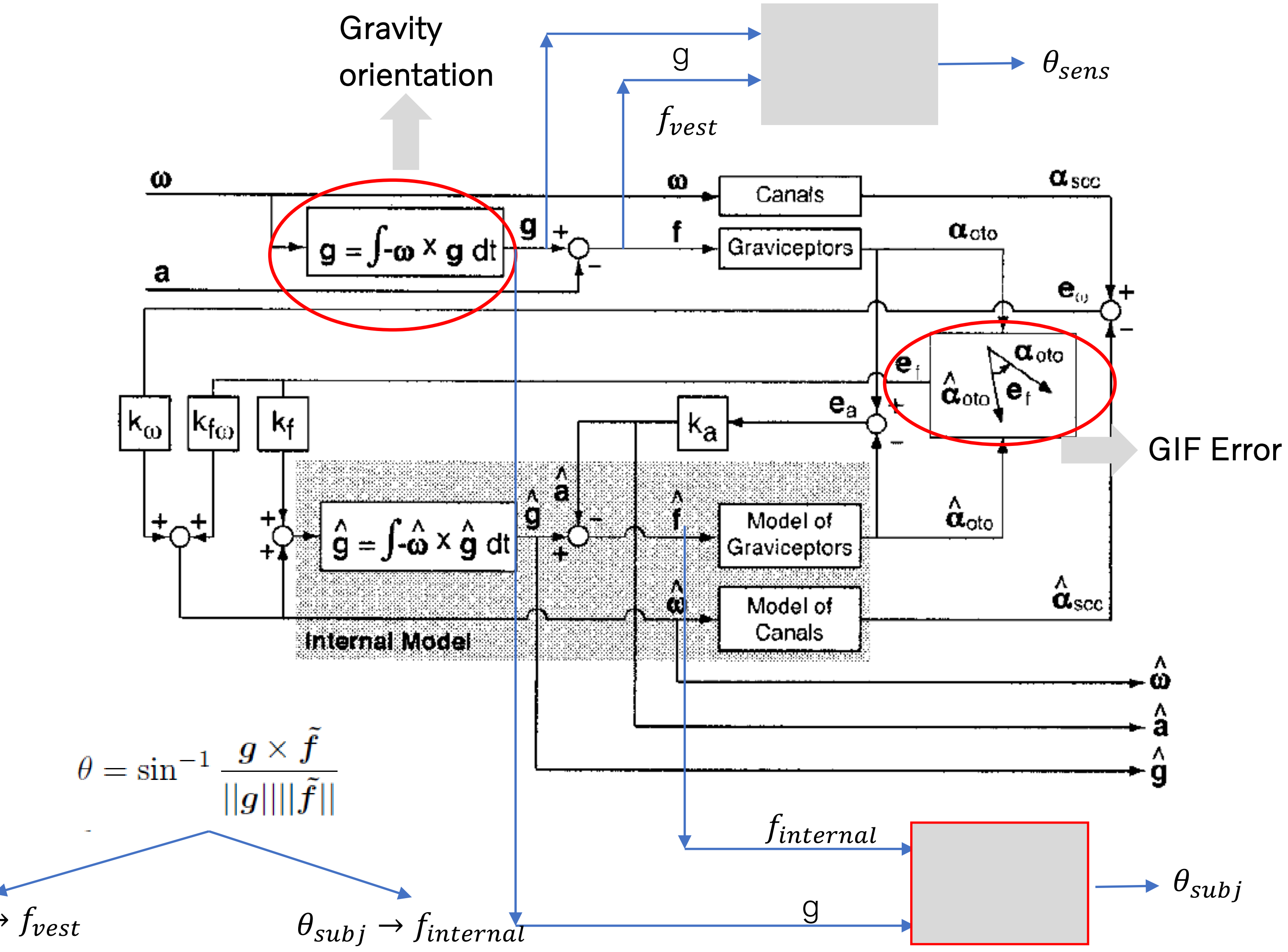

- The model consist of 4 different gains $(k_a, k_\omega, k_{f\omega}, k_f)$ where each weights for the different sensory conflict vectors (e_a, e_f, e_ω).
- **GIF orientation error** represented mathematically *as direction of unit vector perpendicular to plane*
  - $(\frac{\vec{\hat{\alpha}}_{oto}}{|\vec{\hat{\alpha}}_{oto}|} \otimes \frac{\vec{\alpha}_{oto}}{|\vec{\alpha}_{oto}|})$
- **GIF magnitude error** represented as *vector cross product or vector dot product*
  - $sin^{-1}(\frac{\vec{\hat{\alpha}}_{oto}}{|\vec{\hat{\alpha}}_{oto}|} \otimes \frac{\vec{\alpha}_{oto}}{|\vec{\alpha}_{oto}|})$
- The model used the Canals transfer function from **Goldberg and Fernandez (1971).**
- This model was validated against **Roll tilt, Fixed Cab Centrifugation** and **Postrotational Tilt** paradigm.
- According to **Merfeld (2005),** he argued that the simple filtering method proposed by Mayne (1974), does not contribute substantially to human perception of tilt or translation.

VOLVO

Haslwanter Model (2000)

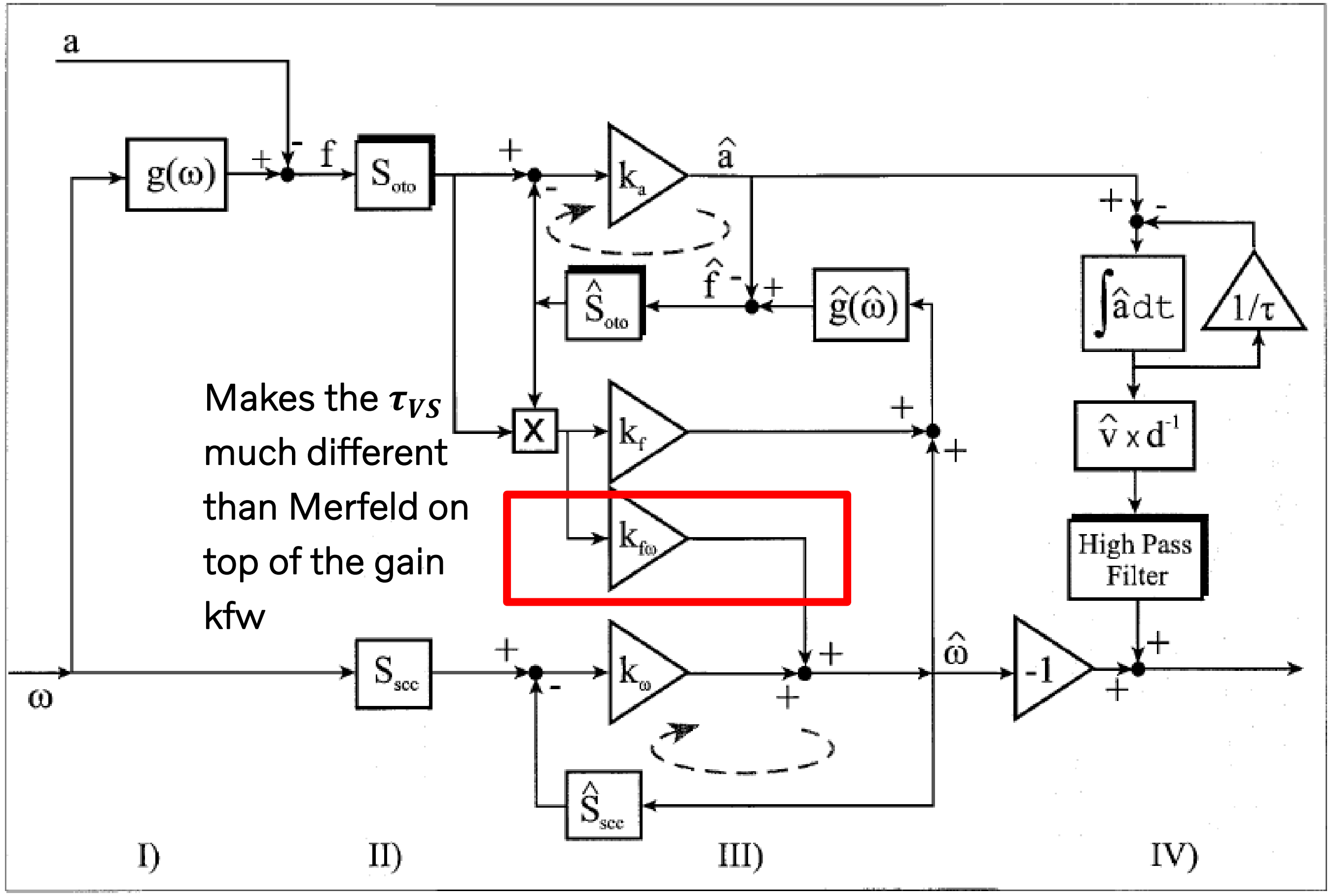

- Haslwanter modified the Merfeld model to fit with the eye movement response during Off-Vertical Axis Rotation (OVAR) experimental tests done on human test subjects.
- The additional component of pitch shear is modeled for Soto block due to utricular macula….

Parameters	Values
k_a	-1 [-]
k_ω	1 [-]
k_f	10 $[\frac{1}{s}]$
$k_{f\omega}$	1 $[\frac{1}{s}]$
τ_{integ}	2 [sec]
$\tau_{highpass}$	0.3 [sec]
d	3

Validation Methods : 1. OVAR test

with our experimental data: k_a=–1, k_f=10, $k_{f\omega}$=1, k_ω=1, τ_d^{scc}=7, τ_a^{scc}=190, τ_{Integ}=2, $\tau_{HighPass}$=0.3, d=3. To run the simulation we

Vingerhoets model

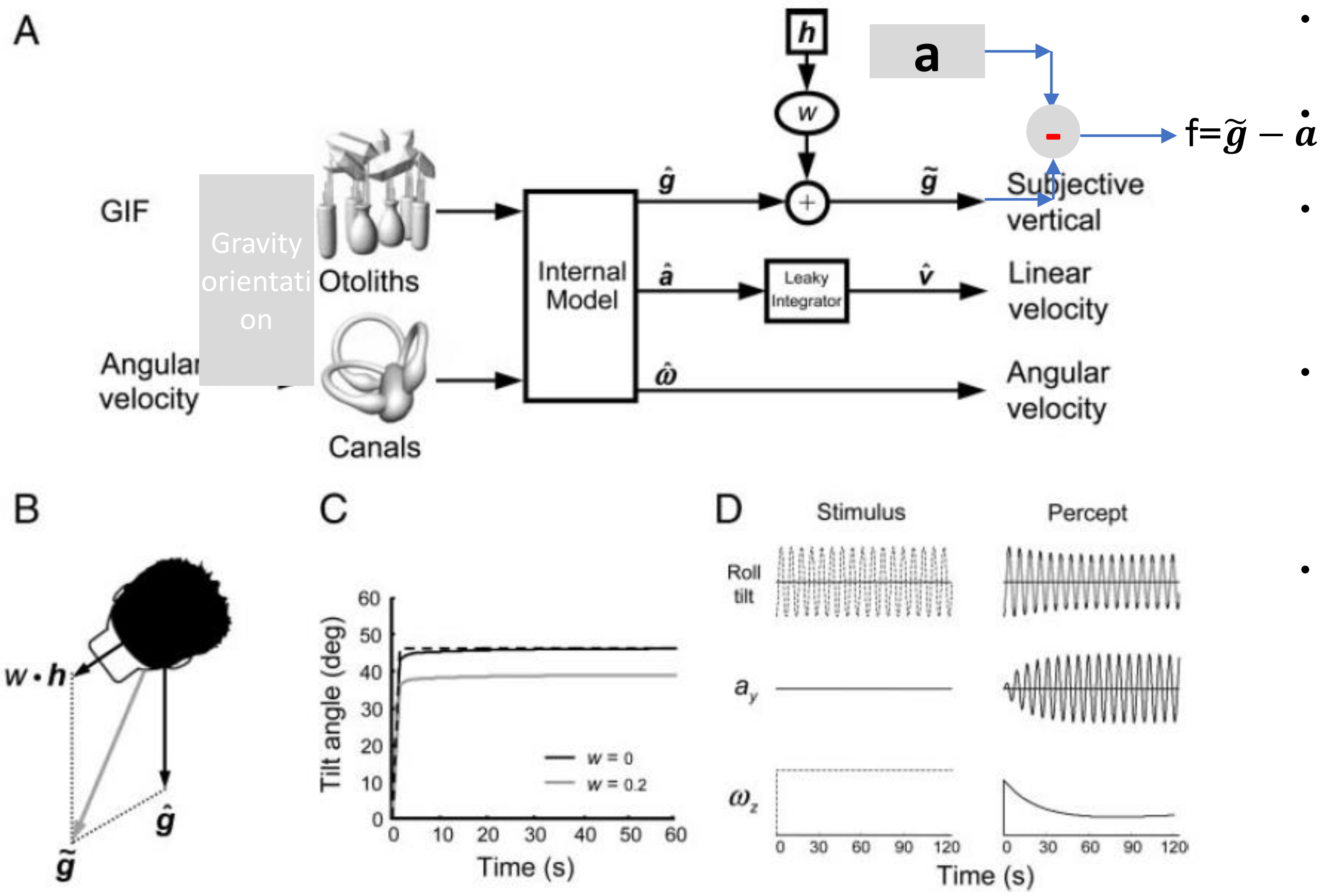

- Model is an adapted version of the model proposed by Merfeld and Zupan (2002).
- A leaky integrator was added to obtain correct predictions of the magnitude of illusory translation during off-vertical axis rotation.
- Our results suggest that the canal– otolith interaction model can explain the SVV data during OVAR when extended by an idiotropic mechanism.
- Contrary to the previous research done by Haslwanter using OVAR test which utilize the motor output (e.g. eye movement response) experimental results to fit the free parameters, the research done by Vingerhoets et al. adapted the Merfeld model using the illusory perception experimental fit.
- In addition to this, to account for subjective visual vertical rotational perception underestimation in static tilt stimulus which is in faster rate and earlier onset of the stimulus perception decay compared to the previous model, Vingerhoets et al. adjust the proposed free parameters while taking into account the existence of leaky integration that exists in their previous model.
- Mathematically, the writer expressed it with an additional term to the internal model output ($\hat{g}$) with an additional term (w$\cdot$ h), a constant weighting coefficient which scales the upright idiotropic head vector assumption to get the subjective visual vertical ($\tilde{g}$).

verticality perception. Inspired by several studies (Dyde et al. 2006; Groen et al. 2002; Mittelstaedt 1983; Zupan and Merfeld 2005; Zupan et al. 2002), we modeled the subjective vertical as a weighted vector sum of the estimated direction of gravity and the direction of the long-body axis ($\tilde{\mathbf{g}} = \hat{\mathbf{g}} + w{\cdot}\mathbf{h}$; see Fig. 1*B*). Parameter *w* is a tilt-independent variable, which represents the relative weights of these two vectors and can vary across subjects. Head vector **h** has virtually no effect on verticality perception when estimated head tilt is small.

$$w = 0.2,\ h \rightarrow \text{head idiotropic vector} \left(= \begin{bmatrix} 0 \\ 0 \\ -9.81 \end{bmatrix} \right)$$

$$\tilde{g} = \hat{g} + w\cdot h = \hat{g} + \begin{bmatrix} 0 \\ 0 \\ -1.962 \end{bmatrix}$$

TABLE 1. *Model performance with two different parameter sets*

	Parameter Values					Fit Residuals (RMSE)	
	k_a	k_f	$k_{f\omega}$	k_ω	τ_{leaky}	Translation and Rotation Data, deg/s	Dynamic SVV Component, deg
Parameters Based On:							
Rotation and translation data	−4	4	8	8	0.06	5.6	5.2
Dynamic SVV component	−4	2	8	2	0.06	8.2	5.1

VOLVO

Newman Model w/ visual inputs

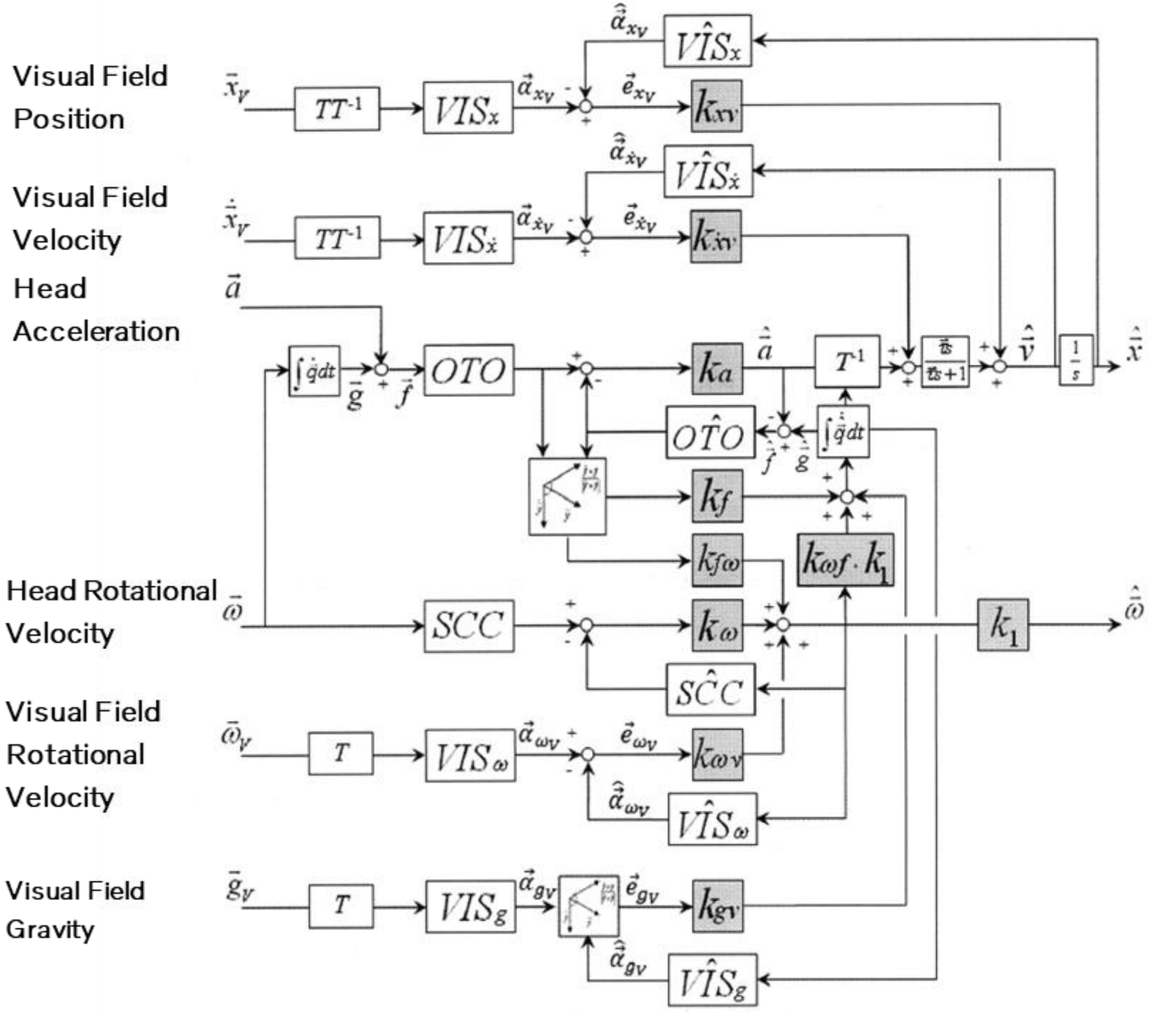

- The model consist of 5 different vestibular gains $(\boldsymbol{k_a}, \boldsymbol{k_\omega}, \boldsymbol{k_{f\omega}}, \boldsymbol{k_{\omega f}}, \boldsymbol{k_f})$ and 4 different visual gains $(\boldsymbol{k_{X_v}}, \boldsymbol{k_{\dot{X}_v}}, \boldsymbol{k_{g_v}}, \boldsymbol{k_{\dot{\omega}_v}})$ where each visual gain weights for the different sensory conflict vectors **$(\boldsymbol{e_{X_v}}, \boldsymbol{e_{\dot{X}_v}}, \boldsymbol{e_{g_v}}, \boldsymbol{e_{\dot{\omega}_v}})$.**
- **GIF error** calculation are done in the same way as **Merfeld (2001)** model did.
- The model used the Canals transfer function from **Goldberg and Fernandez (1971).**
- The gravity vector estimation were done using the quarternion integration method as will be discussed in next page.
- The visual position **($\vec{\boldsymbol{x}}$)** is derived from the **weighted acceleration vector $\hat{\vec{\boldsymbol{a}}}$** which is passed through the 3D leaky integrator filter with time constant **$(\boldsymbol{\tau_X}, \boldsymbol{\tau_Y}, \boldsymbol{\tau_Z})$.**
- The visual inputs were processed hypothetically through the coordinate transformation from **the world to head or the world to the limbic** coordinates system.
- This model was validated against **Cross/Pseudo Coriolis, Fixed Cab Centrifugation, EVAR, OVAR, Forward Acceleration** paradigm.

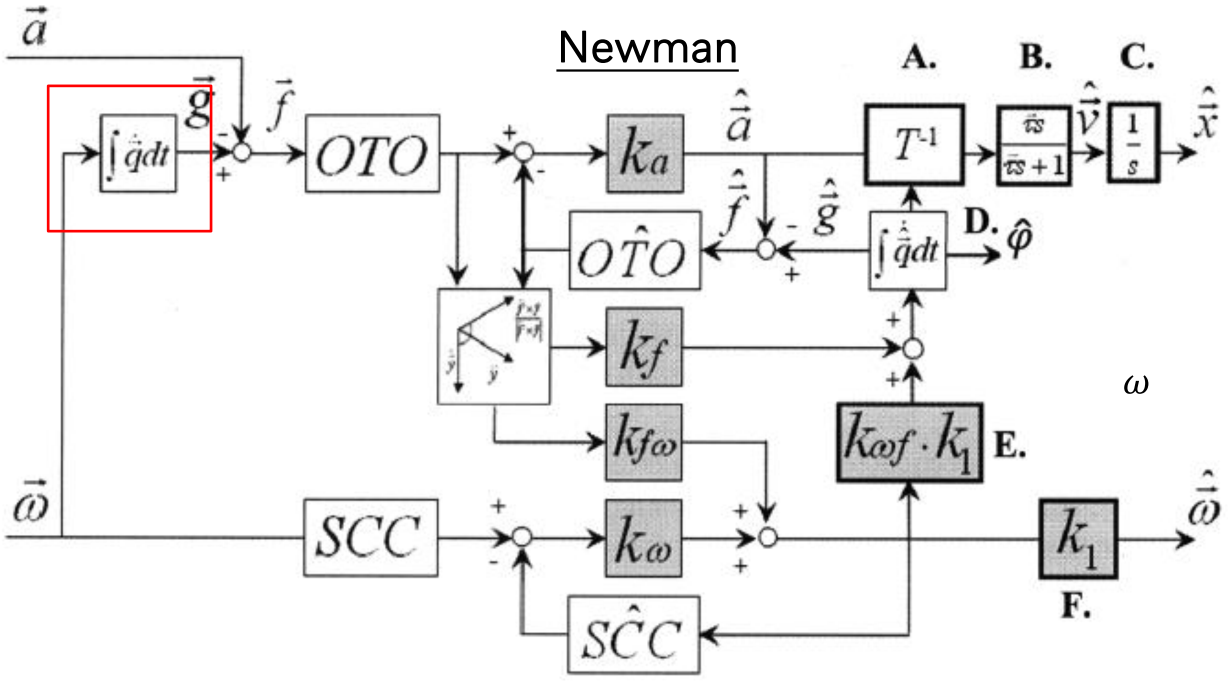

Model Newman Explanation.pdf

Parameters	Values
k_a	-4 [-]
k_ω	8[-]
$k_{f\omega}$	8 [$\frac{1}{sec}$]
k_f	4 [$\frac{1}{sec}$]
$k_{\omega f}$	1
k_1	0.75 [-]
τ	[16.66 16.66 1]^T [sec]

Validation Methods :

1. Linear and angular acceleration steps
2. Postrotatory tilt
3. Constant velocity Earth vertical yaw rotation
4. Somatogravic illusion
   a. Forward linear acceleration on a sled
   b. Fixed and variable radius centrifugation
5. Static and dynamic roll tilt
6. Off-vertical-axis rotation (OVAR)
7. Large amplitude horizontal and vertical sinusoidal displacements
8. Constant velocity Earth vertical yaw rotation in the light
9. Circular vection
10. Somatogravic illusion due to forward linear acceleration in a lighted cabin
11. Forward linear vection
12. Coriolis
13. Pseudo Coriolis
14. Astronaut post-flight illusions
    a. Tilt-Gain
    b. Tilt-Translation

Estimator Models

Kalman Filter (Borah) Model (1979)

- Borah Kalman filter model consists of 25 state vectors which represent the modelling of internal model.
- The conflict between the visual and vestibular output estimation determines the rate of change of the final model output which is adopted from previous research by **Zacharias and Young (1981)**.
- The Kalman filter assumes that the noises are of **Gaussian distributed type** and are divided into the **Process Noise** and **Measurement Noise** which reflects the noise in the vestibular system in processing and measurement dynamic of external stimulation. These noises are tuning parameters for the model.
- The internal model consists of two different model **(Stimulus model and Sensor model)** which determines the perceived bandwidth of the external stimulation and the canal and otolith time constant.
- The internal model is linearized around the initial upright condition which represent a limitation of this model **(not works well for large attitude).**
- According to **Selva and Oman (2012),** Borah model is equal to a higher order version of the Merfeld model from the analysis result of the output rotational velocity of the simplified version of Borah model in fitting the same empirical data.

Simplified Borah 3D Kalman Filter (Selva Thesis)

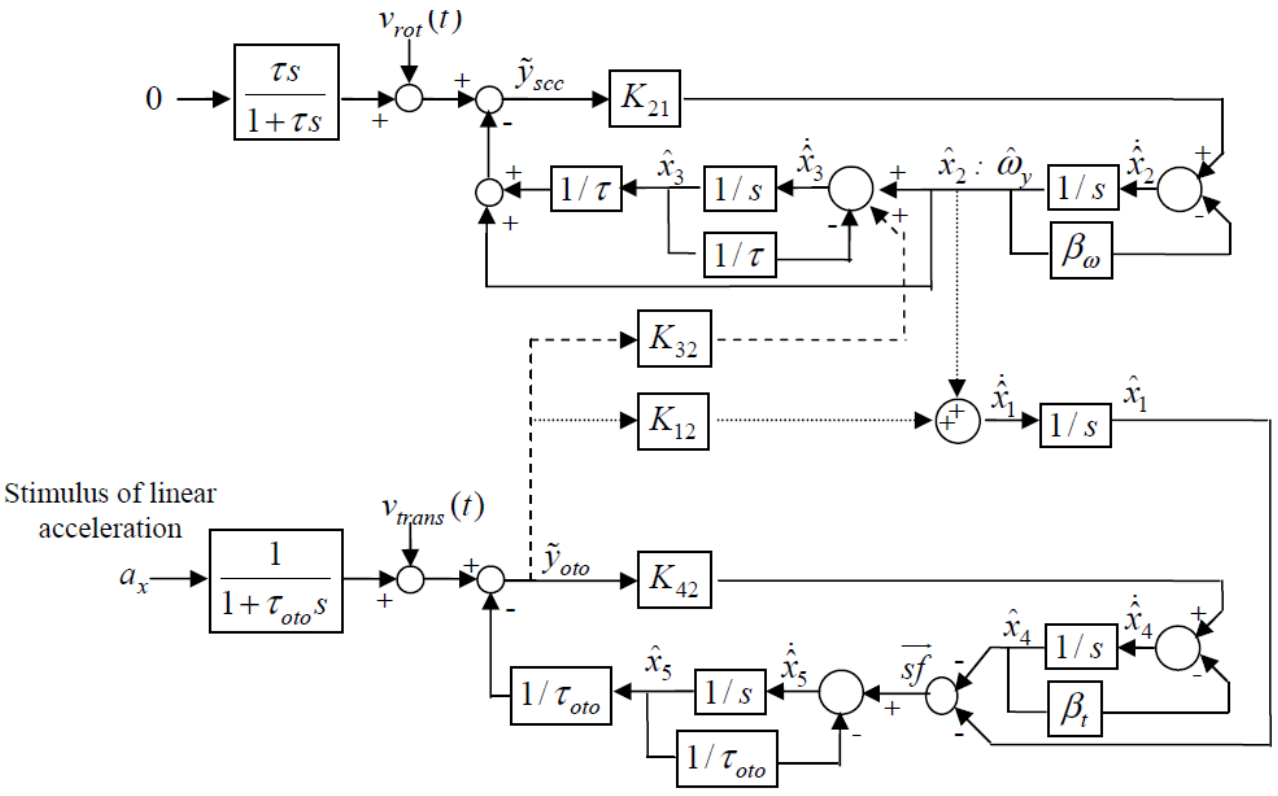

Figure 4.11. *Block diagram of the steady state Kalman filter for the somatogravic illusion. The syste corresponds to a KF with only the four necessary gains.* $\hat{x}_1$, $\hat{x}_2$, *and* $\hat{x}_4$ *correspond to perception c orientation, angular velocity, and linear acceleration, respectively.*

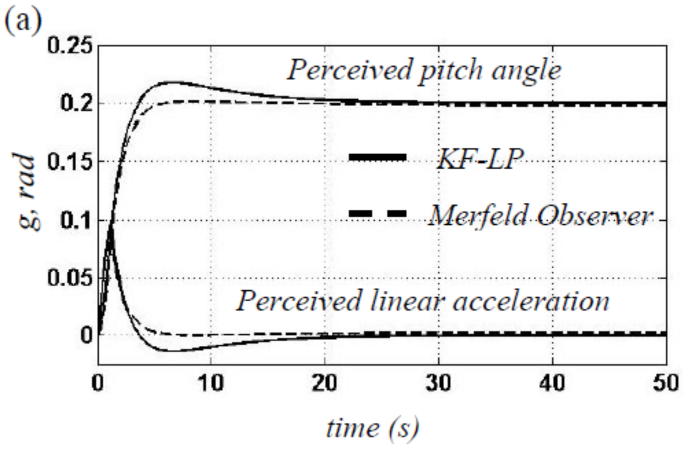

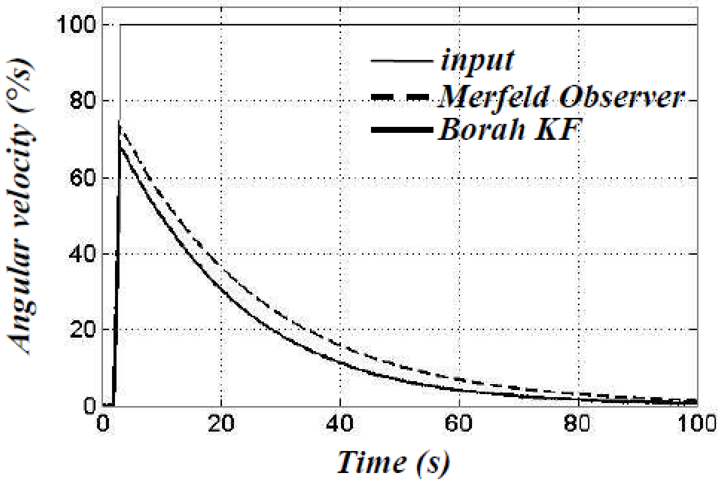

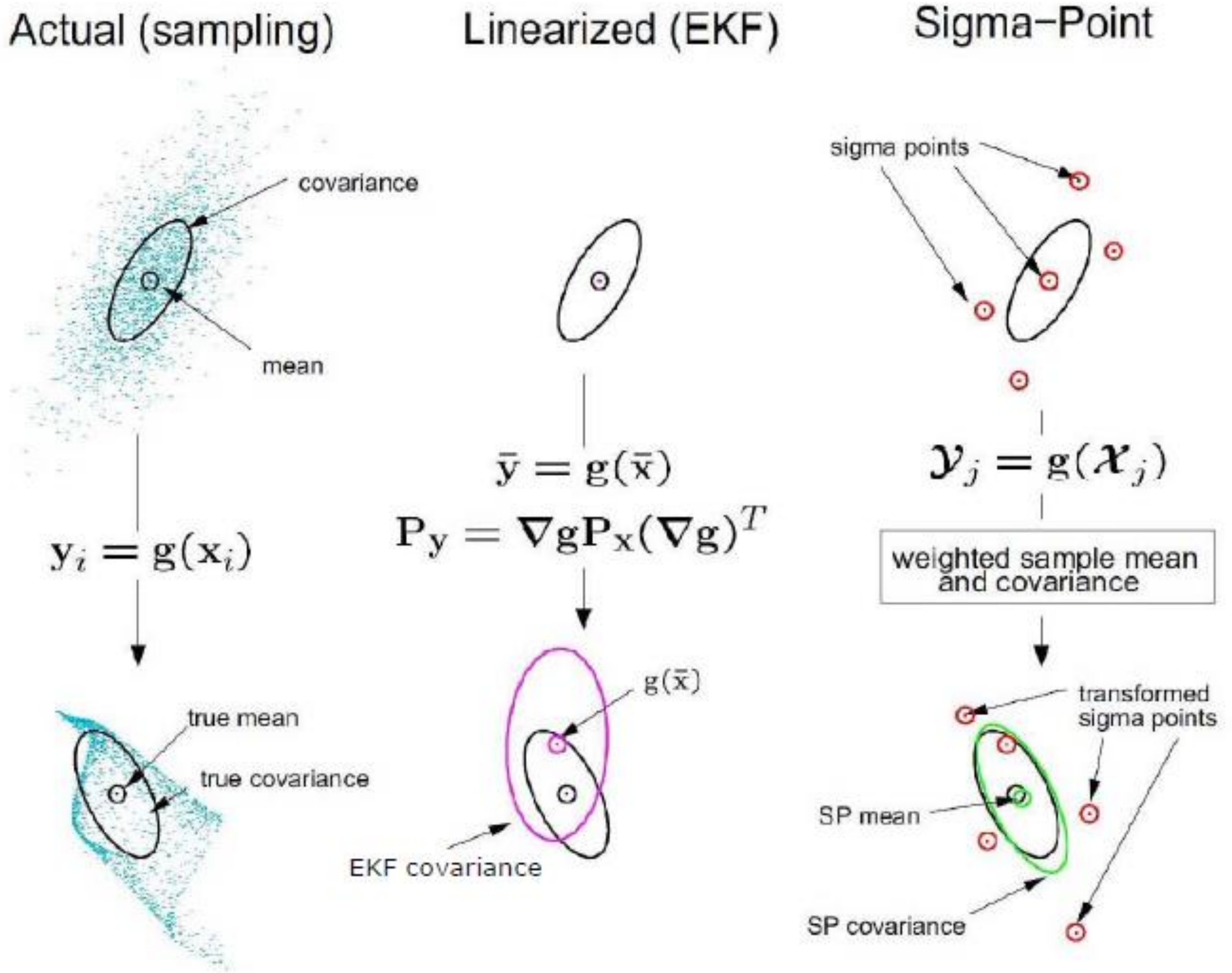

Figure 1.13. *Demonstration of the accuracy of the unscented transformation for mean and covariance propagation. (a) Actual (Monte Carlo approach). (b) First-order linearization (EKF). (c) Sigma point transformation (UKF).*

EKF Pomellet Model (1990)

Algorithm 1: The hybrid extended Kalman filter

1. The dynamic system is given by the following equations:

$$\dot{x} = f(x, u, w, t)$$
$$y_k = h_k(x_k, v_k)$$
$$w(t) \sim (0, Q_c)$$
$$v_k \sim (0, V_k)$$

Selva

2. Initialization

$$\hat{x}_0^+ = E(x_0)$$
$$P_0^+ = E\left[(x_0 - \hat{x}_0^+)(x_0 - \hat{x}_0^+)^T\right]$$

3. For $k = 1, 2, \dots$

(a) Prediction step: integrate the state estimate and its covariance from time $(k-1)^+$ to time k^- as follows:

$$\dot{\hat{x}} = f(\hat{x}, u, 0, t)$$
$$\dot{P} = AP + PA^T + LQ_cL^T$$

where $A = \left.\frac{\partial f}{\partial x}\right|_{\hat{x}}$, $L = \left.\frac{\partial f}{\partial w}\right|_{\hat{x}}$. This integration begins with $\hat{x} = \hat{x}_{k-1}^+$ and $P = P_{k-1}^+$. At the end of this integration we have $\hat{x} = \hat{x}_k^-$ and $P = P_k^-$.

(b) Correction step: at time k, incorporate the measurement y_k into the state estimate and estimation covariance:

$$K_k = P_k^- H_k^T (H_k P_k^- H_k^T + V_k)^{-1}$$
$$\hat{x}_k^+ = \hat{x}_k^- + K_k\left[y_k - h_k(\hat{x}_k^-, t)\right]$$
$$P_k^+ = (I - K_k H_k) P_k^- (I - K_k H_k)^T + K_k V_k K_k^T$$

where H_k is the partial derivatives of $h_k(x_k, v_k)$ with respect to x_k, and is evaluated at $\hat{x}_k^-$.

- The transfer function used in the model is

$$TF_{oto} = \frac{1}{(s+0.1)(s+100)}, \qquad TF_{SCC} = \frac{80.6s^2}{(80.6s+1)(6s+1)}$$

- The gravity vector estimation were done using the quarternion integration method.
- The visual contribution is divided into two separate different pathway, **Focal and Ambient**.
- The vestibular and visual pathway both include a threshold and saturation which comes from previous experimental results **by Barson (1989), Gillingham (1986) and Young (1978).**
- The model was validated using **Fixed Radius Centrifugation, EVAR and Forward Acceleration motion paradigm.**
- **The model claimed to gave a better accuracy of estimation of the linear velocity, acceleration and pitch illusory sensation in the dark compared to the previous model by Borah.**
- **The model, however, could not simulate the delay phenomena in vection experimental results. Hence, these inadequacies of the visual component might be improved in the future**.

EKF Pomellet Model (1990)

Algorithm 1: The hybrid extended Kalman filter

1. The dynamic system is given by the following equations:

$$\dot{x} = f(x,u,w,t)$$
$$y_k = h_k(x_k, v_k)$$
$$w(t) \sim (0, Q_c)$$
$$v_k \sim (0, V_k)$$

2. Initialization

$$\hat{x}_0^+ = E(x_0)$$
$$P_0^+ = E\left[(x_0 - \hat{x}_0^+)(x_0 - \hat{x}_0^+)^T\right]$$

3. For $k = 1, 2, \ldots$

(a) Prediction step: integrate the state estimate and its covariance from time $(k-1)^+$ to time k^- as follows:

$$\dot{\hat{x}} = f(\hat{x}, u, 0, t)$$
$$\dot{P} = AP + PA^T + LQ_cL^T$$

where $A = \left.\frac{\partial f}{\partial x}\right|_{\hat{x}}$, $L = \left.\frac{\partial f}{\partial w}\right|_{\hat{x}}$. This integration begins with $\hat{x} = \hat{x}_{k-1}^+$ and $P = P_{k-1}^+$. At the end of this integration we have $\hat{x} = \hat{x}_k^-$ and $P = P_k^-$.

(b) Correction step: at time k, incorporate the measurement y_k into the state estimate and estimation covariance:

$$K_k = P_k^- H_k^T (H_k P_k^- H_k^T + V_k)^{-1}$$
$$\hat{x}_k^+ = \hat{x}_k^- + K_k\left[y_k - h_k(\hat{x}_k^-, t)\right]$$
$$P_k^+ = (I - K_k H_k) P_k^- (I - K_k H_k)^T + K_k V_k K_k^T$$

where H_k is the partial derivatives of $h_k(x_k, v_k)$ with respect to x_k, and is evaluated at $\hat{x}_k^-$.

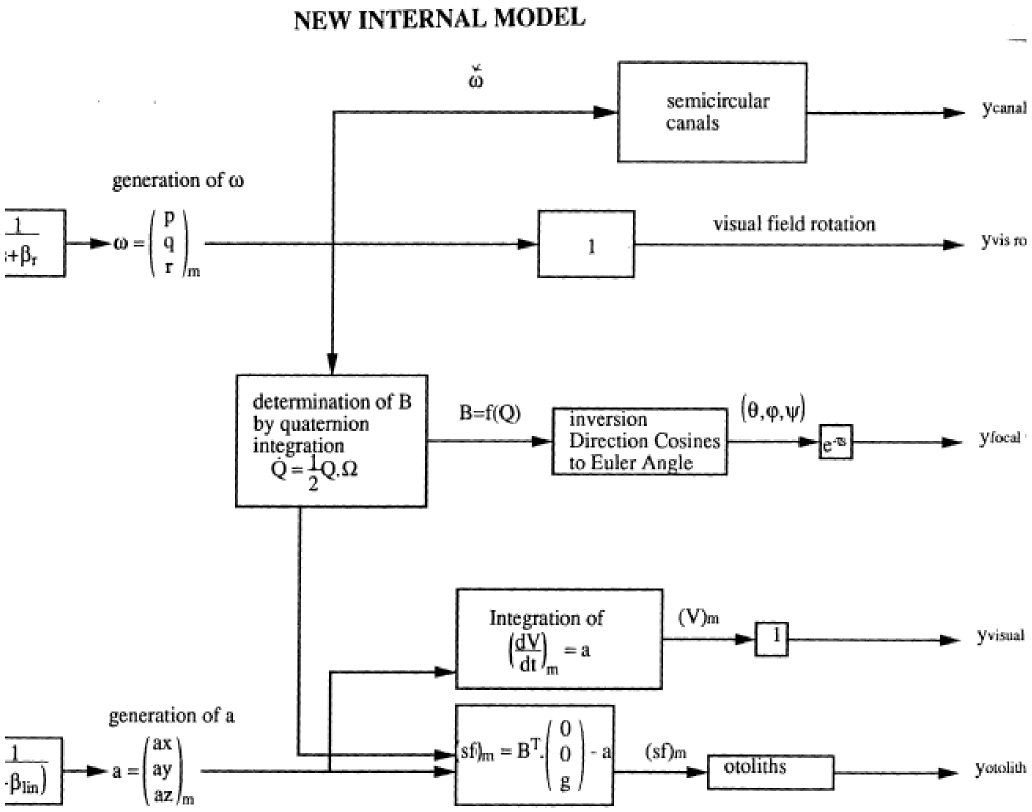

UKF Selva model (2009)

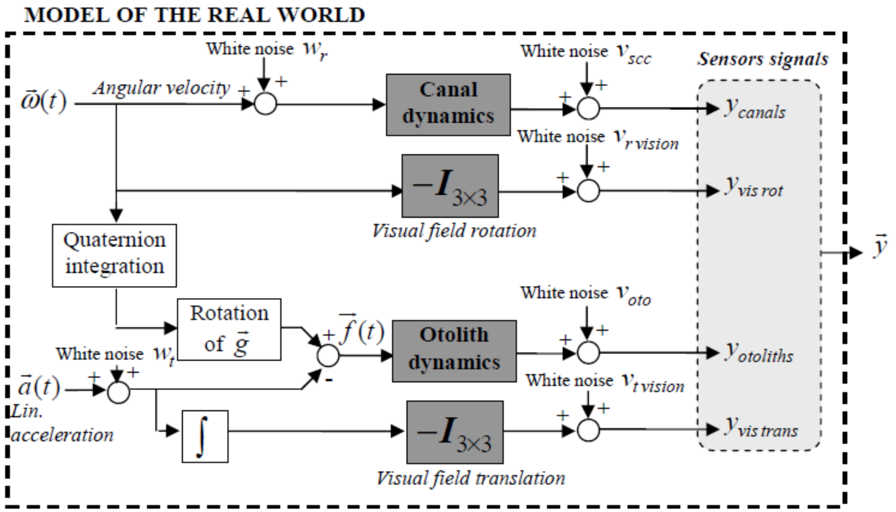

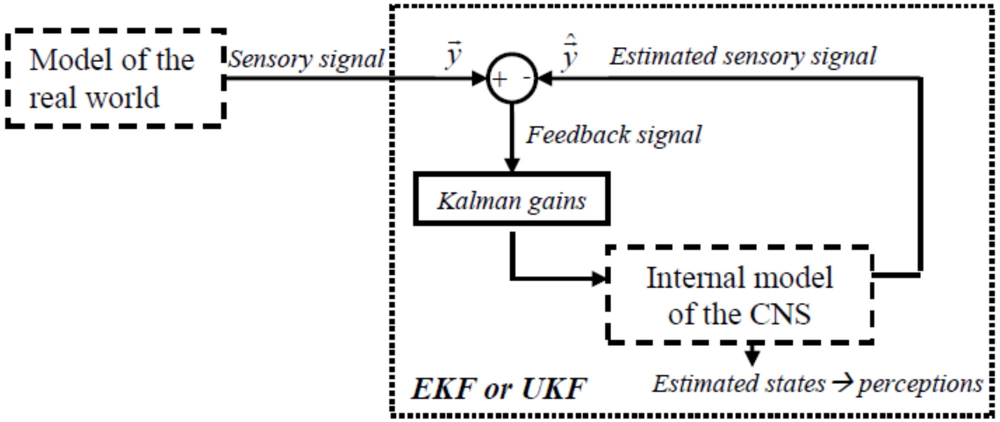

- The model utilized a Gaussian distribution of state noise. However, it use an additional minimal set of deterministic chosen sample points (sigma points).
- The model claim that UKF formulation will allow statistical accuracy of the posterior distribution to increase into the 2nd order against 1st order in EKF formulation.
- The model used the Canals and Otoliths transfer function from **Telban and Cardullo (2005).**
- **Canal and Otolith Dynamics are different than Pomellet Model (1990).**
- The gravity vector estimation were done using the quarternion integration method.
- The model also utilized a fictitious process noise for the quarternion to reduce numerical instabilities with value $Q_{quat} = 10^{-5}$.
- The model excludes the visual eye movement component as well as the relationship between the vestibular sensors and the vestibulo ocular-reflex.
- The model was validated using **Pseudo Coriolis, EVAR and Forward Acceleration motion paradigm.**

UKF Selva model (2009)

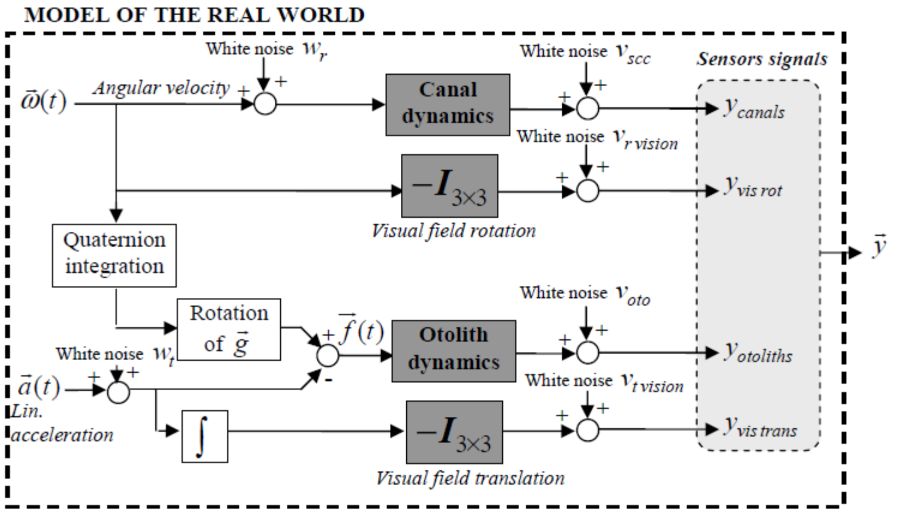

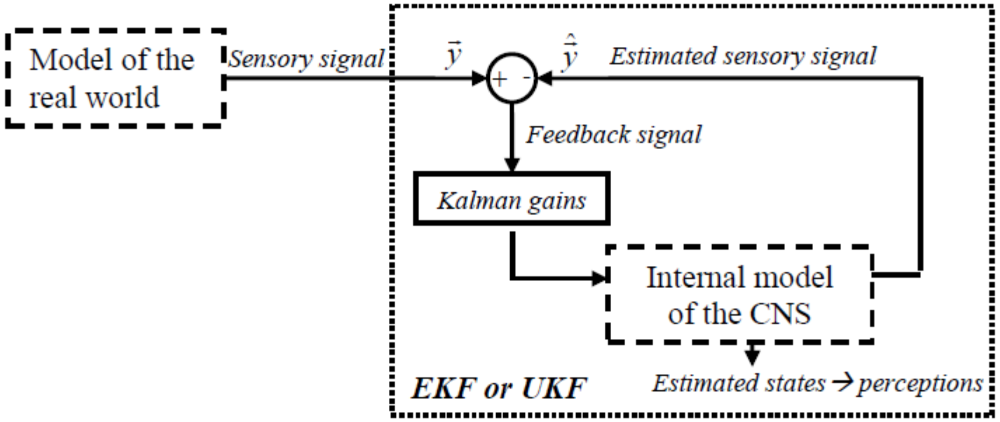

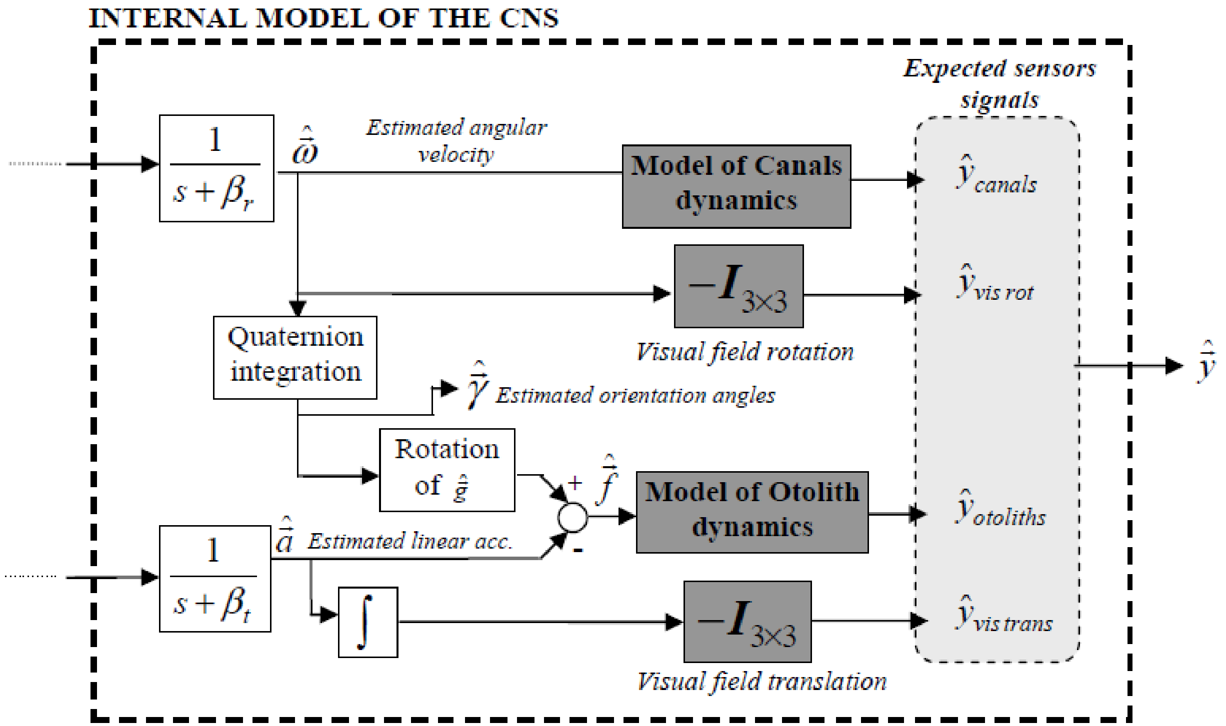

Algorithm 2: The hybrid unscented Kalman filter

Initialization

$$\hat{x}_0^+ = E(x_0)$$

$$P_0^+ = E\left[(x_0 - \hat{x}_0^+)(x_0 - \hat{x}_0^+)^T\right]$$

For $k = 1, 2, ...$

1. Calculate sigma-points:

$$X_{k-1} = \left[\hat{x}_{k-1} \ \cdots \ \hat{x}_{k-1}\right] + \sqrt{n+\lambda}\left[0 \ \ \sqrt{P_{k-1}} \ \ -\sqrt{P_{k-1}}\right]$$

2. Time update equations: integrate the state estimate and its covariance :

$$\dot{\hat{x}} = f(X(t))W^m$$

$$\dot{P}(t) = X(t)Wf^T(X(t)) + f(X(t))WX^T(t) + Q_c$$

Where $\rightarrow W^m = \left[w_0^m \ \cdots \ w_{2n}^m\right]^T$,

$$\rightarrow W = \left(I - \left[W^m \cdots W^m\right]\right) \times diag\left(w_0^c \ \cdots \ w_{2n}^c\right) \times \left(I - \left[W^m \cdots W^m\right]\right)^T.$$

The predicted mean and covariance are given as $\hat{x}_k^- = \hat{x}(t_k)$ and $P_k^- = P(t_k)$

3. Correction step: measurement update equations

(a) regenerate 2n+1 sigma points with appropriate changes since the current best guess for the mean and covariance of x_k are $\hat{x}_k^-$ and P_k^-

(b) Use the nonlinear measurement equation to transform the sigma-points into predicted measurements:

$$Y_k = h(X_k, t_k)$$

(c) Compute the predicted measurement vector from the transformed sigma-points:

$$\hat{y}_k^- = \sum_{i=0}^{2n} w_i^m Y_k^i$$

(d) Estimate the covariance of the predicted measurement

$$P_y = \sum_{i=0}^{2n} w_i^c (Y_k^i - \hat{y}_k^-)(Y_k^i - \hat{y}_k^-)^T$$

(e) Estimate the cross-covariance between $\hat{x}_k^-$ and $\hat{y}_k$:

$$P_{xy} = \sum_{i=0}^{2n} w_i^c (X_k^i - \hat{x}_k^-)(Y_k^i - \hat{y}_k^-)^T$$

(f) The measurement update can be performed using the normal Kalman filter equations:

$$K_k = P_{xy}P_y^{-1}$$

$$\hat{x}_k^+ = \hat{x}_k^- + K_k(y_k - \hat{y}_k)$$

$$P_k^+ = P_k^- - K_k P_y K_k^T$$

The Role of Internal Noise in Self-Motion Perception by Jacek Filip Khan (2016) for Laurens Particle Filter (2007)

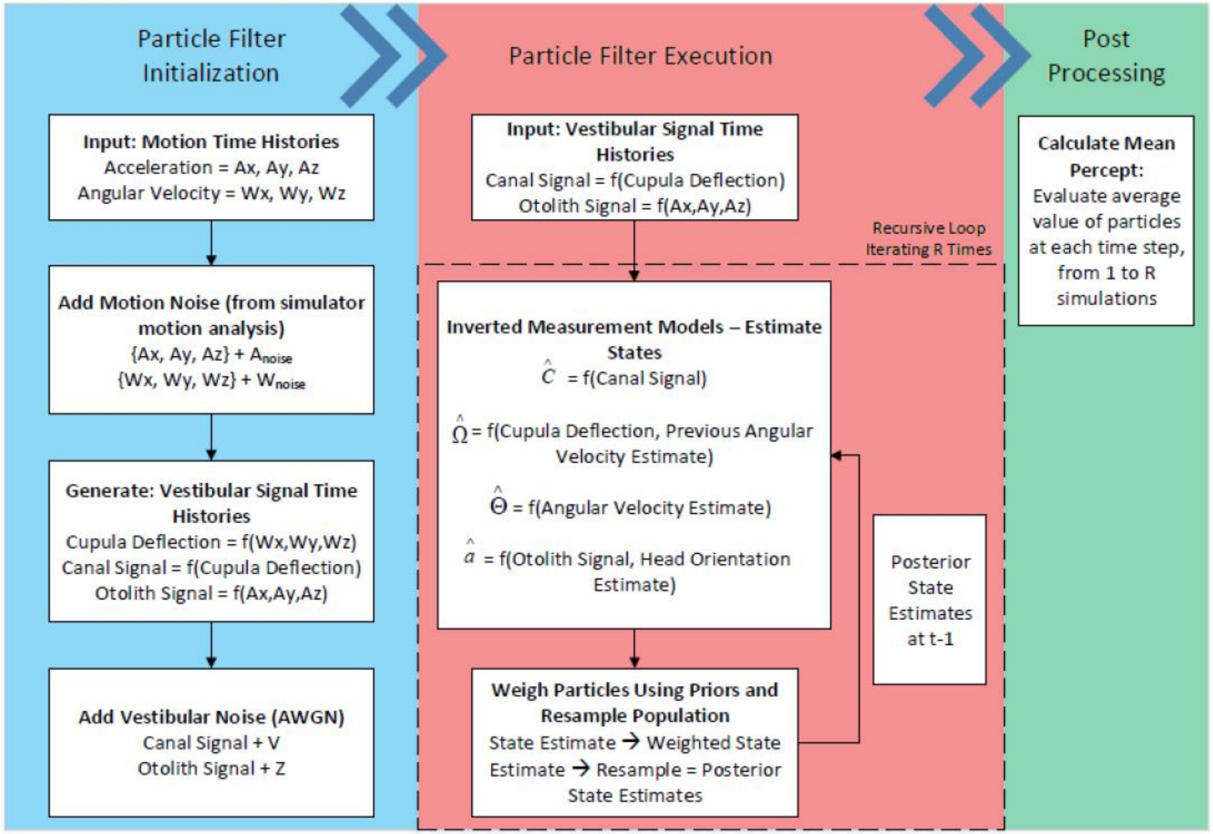

Figure 3.2: Motion perception particle filter block diagram.

Irmak (2022) for Laurens Particle Filter (2007)

Forward Propagation

$$\left\{\begin{array}{l} C_t^i = V_{t-1} - w_t^i \\ \boldsymbol{\omega}_t^i = \boldsymbol{\omega}_{t-1}^i - T_{can}^{-1}\frac{C_t^i \delta t}{T_c} - T_{can}^{-1}(C_t^i - C_{t-1}^i) \\ \Theta_t^i = \Theta_{t-1}^i R(\boldsymbol{\omega}_t^i \delta t) \\ A_t^i = G - \Theta_t^i F_t \end{array}\right\}$$

Prior Distribution

$$\bar{x} = \left\{\begin{array}{c} C_t^i \\ \boldsymbol{\omega}_t^i \\ \Theta_t^i \\ A_t^i \end{array}\right\} \longrightarrow$$

Likelihood Weighting

$$\left\{\begin{array}{l} w_t^i \propto P(x_t^i | x_{t-1}^i) \\ P(x_t^i | x_{t-1}^i) = P(A_t) P(\Omega_t) \\ P(A_t) \propto N_{|A_t|, 0, \sigma_A} \\ P(\boldsymbol{\omega}_t) \propto N_{|\boldsymbol{\omega}_t|, 0, \sigma_\omega} \end{array}\right\}$$

Posterior Distribution

$$x = \left\{\begin{array}{c} C_t^i \\ \boldsymbol{\omega}_t^i \\ \Theta_t^i \\ A_t^i \end{array}\right\} \longrightarrow$$

Fig. 5.4 The Particle Filter model. It is parameterized by: the weighting factor w_t^i given by a multiplication of Gaussian priors (of mean zero and variance σ_A and σ_ω) on the inertial acceleration $P(\vec{A}_t)$ and angular velocity $P(\omega_t)$, the head-to-canal transformation matrix T_{can}^{-1}, the integration time step δt and the canal time constant T_c

Motion Sickness Models

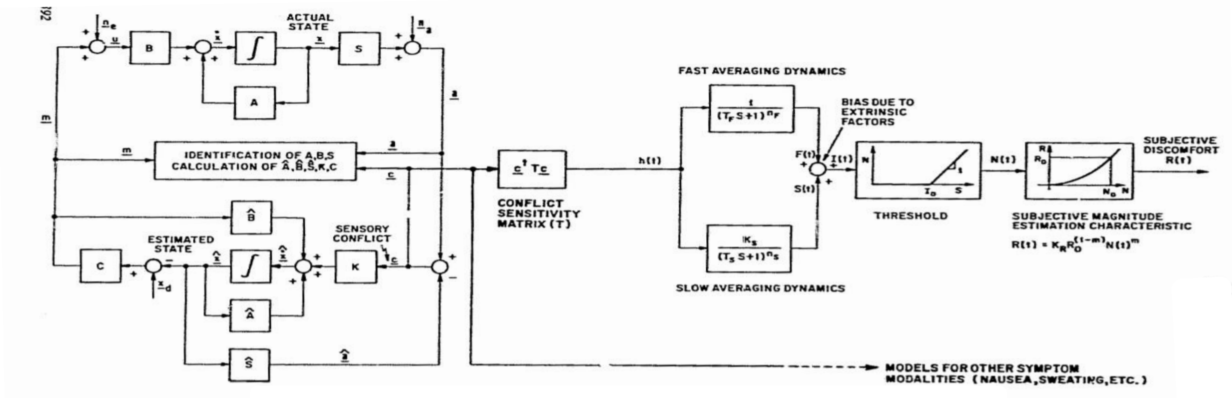

(a). Oman Heuristic model

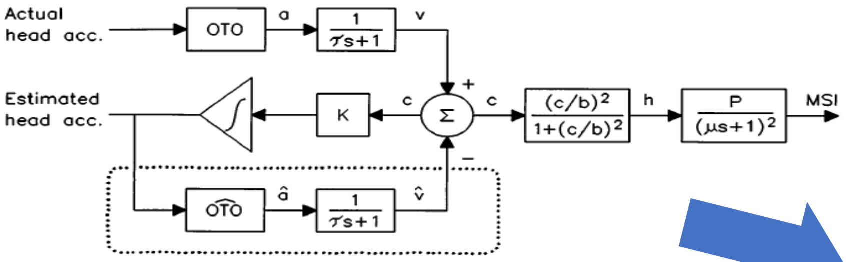

(b). Bos and Bles model

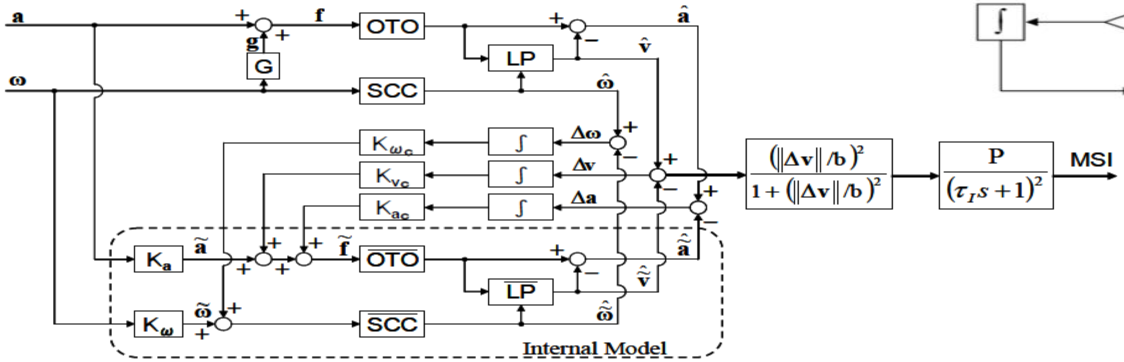

(c). Wada model

To keep the internal model similar to the true dynamics, we also included a mechanism by which the relative orientation of estimated gravity ("gravity storage") is rotated. Similar to the actual body dynamics calculations, we implemented a quaternion integrator[7] ($\int \hat{\dot{\omega}}\, dt \rightarrow \hat{\vec{g}}$) to represent this hypothesized neural process.

Merfeld Says Wada Adopt

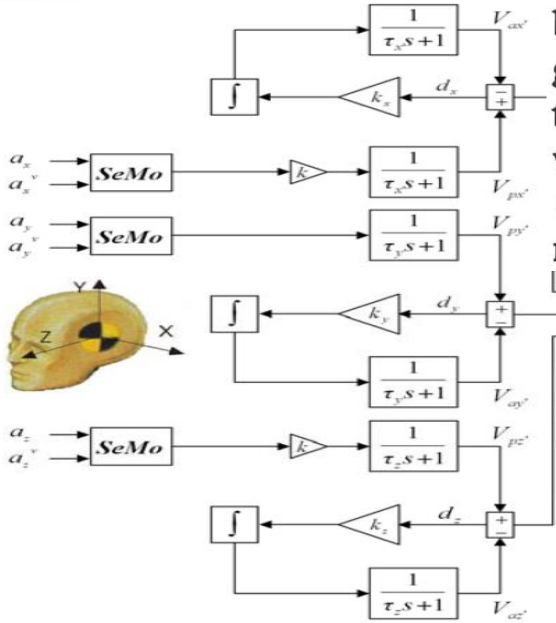


(d). UniPG model

- LP filtering in Wada and Bos-Bles for the gravity vector estimation were done using the **Mayne's Principle (1974)**.
- For Bos and Bles, in comparison to Wada, there is no gravity orientation calculation **block G.**

Wada Internal model Extension (1)

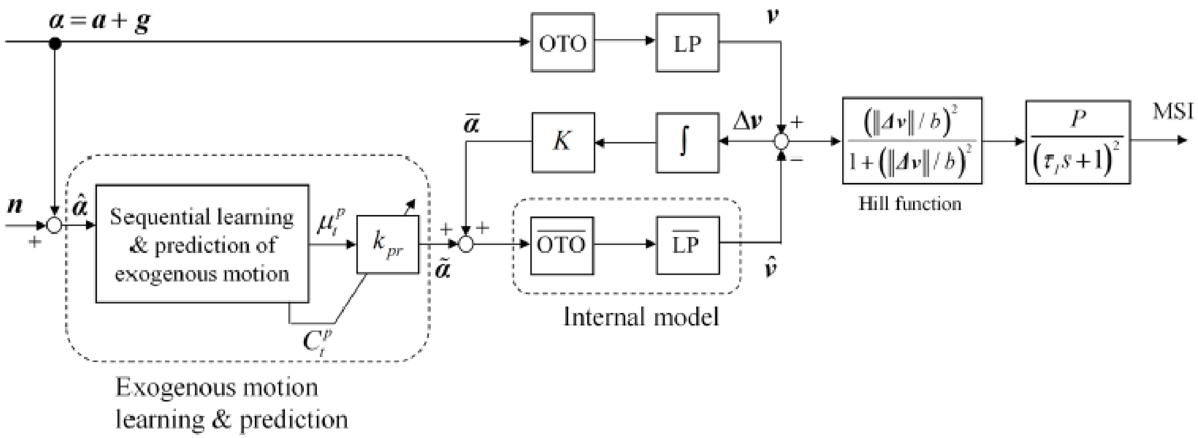

TABLE 1 | Model parameters.

τ[s]	τ_l [s]	K	b [m/s²]	P [%]
2.0	720	5.0	0.5	85.0

Wada (2021)

- The model basically follow the structure of the previous **Wada model (2007)** with additional sequential learning block.
- The learning block is based on the Recursive Gaussian Process Regression method by **Huber (2014)** and the input vectors X definition is based on **Snelson and Ghahramani (2006).**
- The RGPR implementation is based on the principle of Weak anticipation **(Dubois (2003))** of the future states which could mathematically be represented as recursive system below

$$\mathbf{x}(t+1) = \mathbf{R}(\ldots, \mathbf{x}(t-2), \mathbf{x}(t-1), \mathbf{x}(t); \mathbf{p})$$

R → Recursive Function

X(t+1) → Future states of system

X(t-2),X(t-1),X(t) → Past and Present states

Test Method 1 (Earth Vertical Axis Rotation)

- The subjects were seated in a test drum with no light inside and rotated with acceleration/deceleration of 1 deg/s^2 and peak magnitude of 60 deg/s after 2 seconds of stimulation.
- The perception were calculated using the Video-oculography attached on the skin close to the eye such that eye movement could be recorded and rotational Vestibulo-Ocular Reflex (rVOR) magnitude could be measured.
- From the VOR datas, the rotational velocity perception could be inferred as it is theoretically defined as the compensatory movement in the opposite direction of movement of head.
- The velocity storage time constant could be observed by calculating the time that it takes for the rotational velocity perception to decay to 36.8% of the peak value during trapezoidal input stimulus which is done in the Earth Vertical Axis Rotation (EVAR) tests.

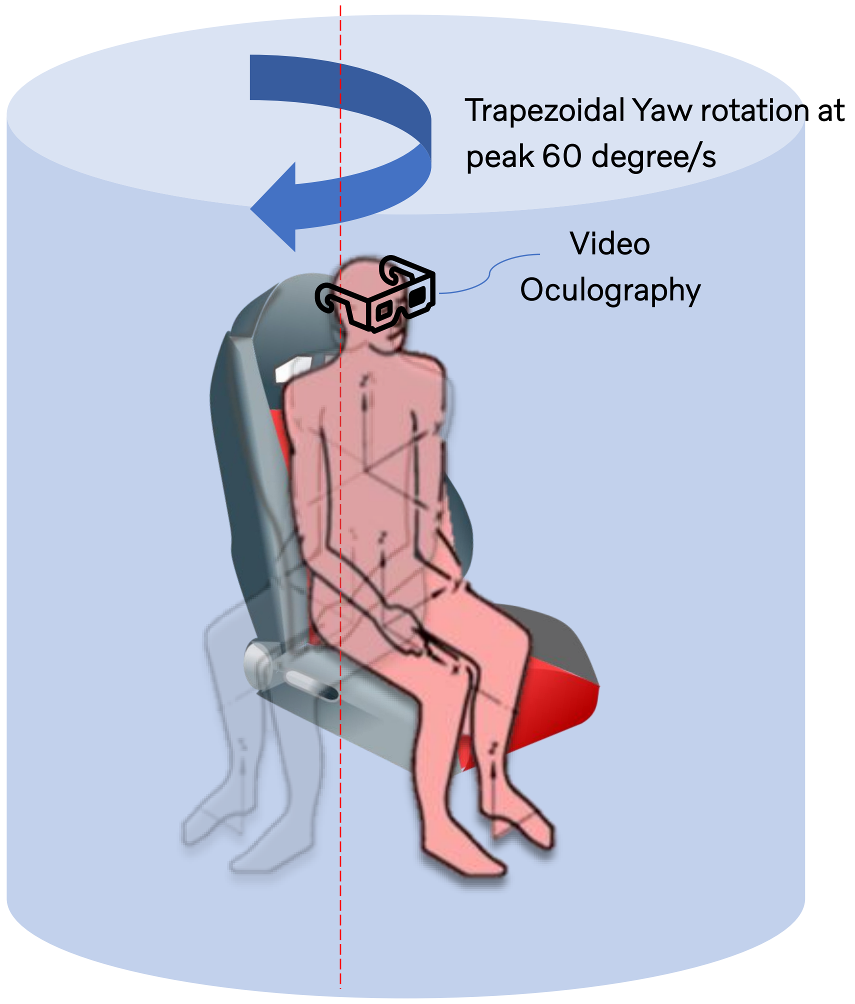

Drum in Darkness Setup

Velocity Storage Time Constant (τ_{VS})

- Velocity Storage refers to mechanism that when the sensed perception afferents from cupula were passed to the CNS, they were processed with filters which has certain time delay constant of leaky integrator due to the neural storage hence giving the output of prolonged reflexive eye movements which improves the compensatory response to low-frequency head rotations.
- It is hypothesized that the time constant of velocity storage influence the motion sickness level experience.
- The concept of the velocity storage mechanism which mostly hypothesized to be present in cerebellar nodulus and uvula by Raphan et al. (1977) has been further developed by Okada et al. (1999) which have suggested that this velocity storage mechanism is also present at higher-level cortical processes such as in rotational self-motion perception.
- The time constant of the velocity storage has been differing in the literature, as Dimitri et al. (2001) proposed 23.6 seconds in yaw-direction, **Bertolini et al. (2012) proposed 17.4 seconds in yaw-direction** and 5.3 seconds in pitch-direction.
- The velocity storage time constant varies with age, diseases, stimulus velocity. It is also noted by the study that there is a trade-off in the brain regarding the accuracy and precision (e.g. noises due to perceptual thresholds, VOR variability and postural responses) (Karmali, 2019). Thus, the time constant is supposed to be shorter in the higher stimulus amplitude condition while VOR variability is supposed to be increased according to (Nouri and Karmali, 2018).

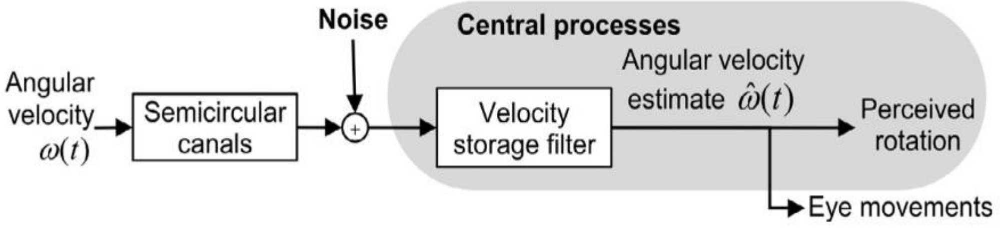

Cited from : From Karmali (2019), "The velocity storage time constant : Balancing between accuracy and precision"

Test Method 2 (Fixed Radius Centrifugation)

- The subjects were seated in a centrifugation machine which has a distance 0.54 m from the center of rotation.
- They were rotated in the clockwise direction with a trapezoidal stimulus with acceleration/deceleration of 1 deg/s^2 and constant peak magnitude of 250 deg/s after 10 seconds. The experiment continue for a total duration of 140 seconds.
- The test setup also generated centripetal acceleration which is proportional to the rotational velocity stimulus and the radius from center of rotation.
- During the test, the participant were tasked to fine tune a visual LED light bar using a button, so that it is parallel to their perceived world horizontal, during the course of the test.
- The subjective vertical time constant could be observed by calculating the time it takes to reach the magnitude of 63.2% of the steady-state final condition during the Fixed Radius Centrifugation (FRC) test.

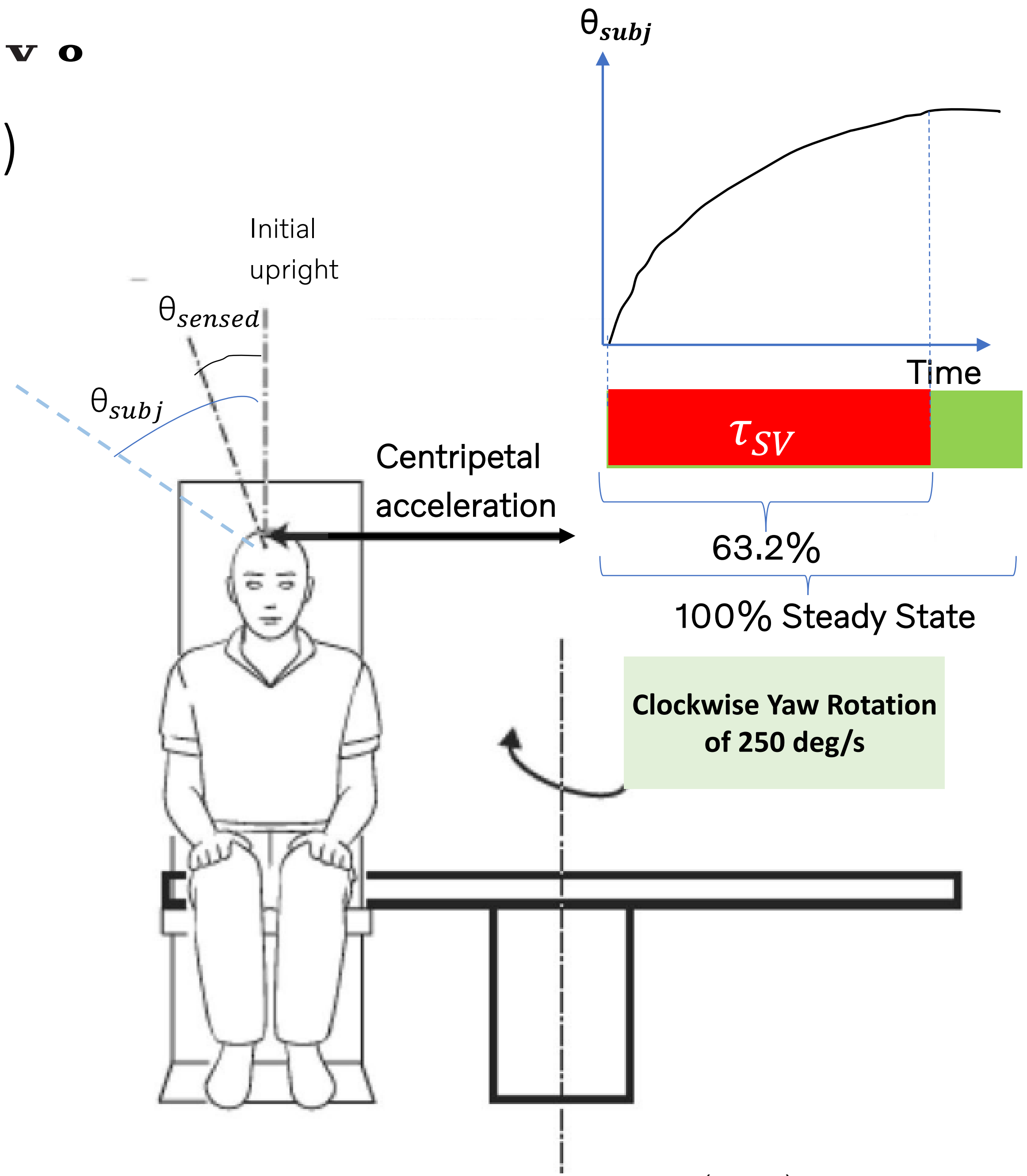

Adapted from Clement et al. (2022) ,
“Effects of motion paradigm on human perception of tilt and translation”

Result for Velocity Storage Time Constant (τ_{VS})

- <u>Revised method 2 (63.2% decay magnitude)</u>
- τ_{VS}=17 s (Merfeld)
- τ_{VS}= 13.4 s (Haslwanter)
- τ_{VS}= 27.1 s (Vingerhoets)
- τ_{VS}= 26.1 s (Newman)
- τ_{VS}= 16.7 s (Selva)
- τ_{VS}= 20.8 s (Pomellet)

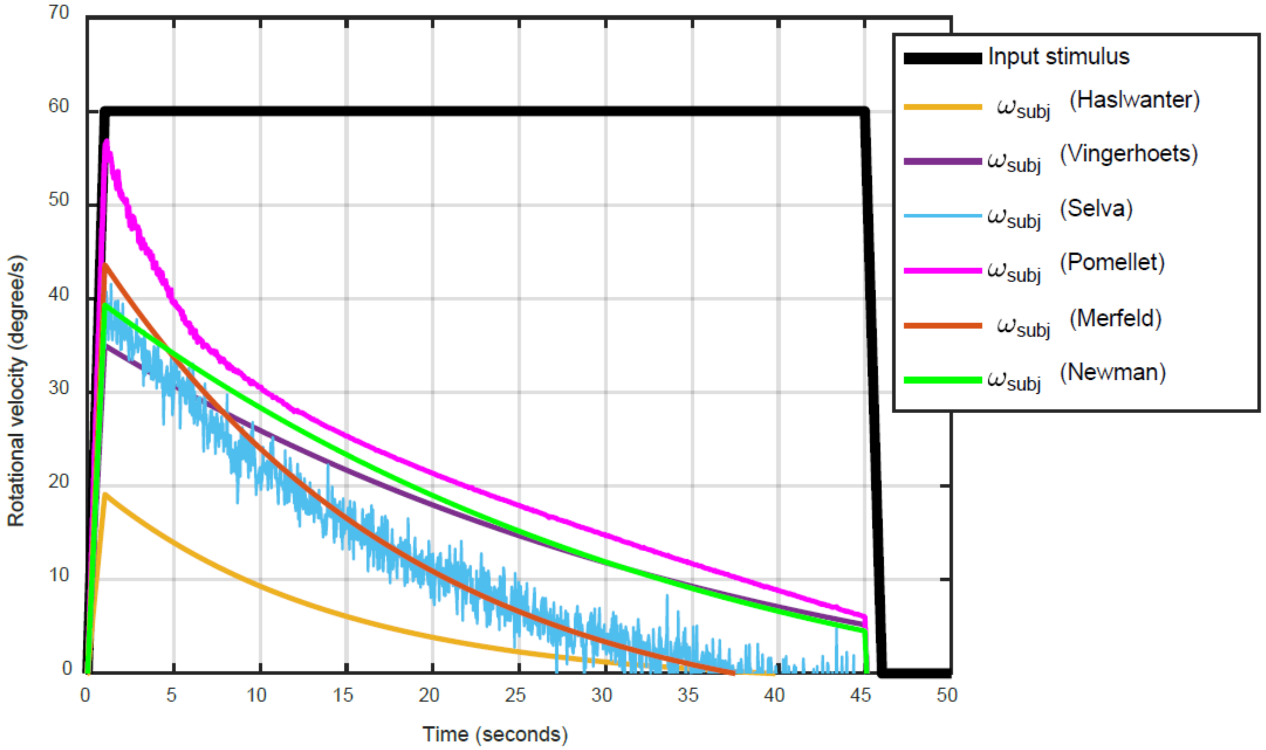

Result for Subjective Vertical Time Constant (τ_{SV})

- **Merfeld and Newman's models give the closest resemblance to the experimental result of average 28.1 s.**
- Wada model could not follow the experimental result perception but could simulate the sensed GIF tilt perfectly.
- The rest of the models while it is less accurate with respect to the average, still in the range of the standard deviation of the experimental results indicated in Merfeld (2001).

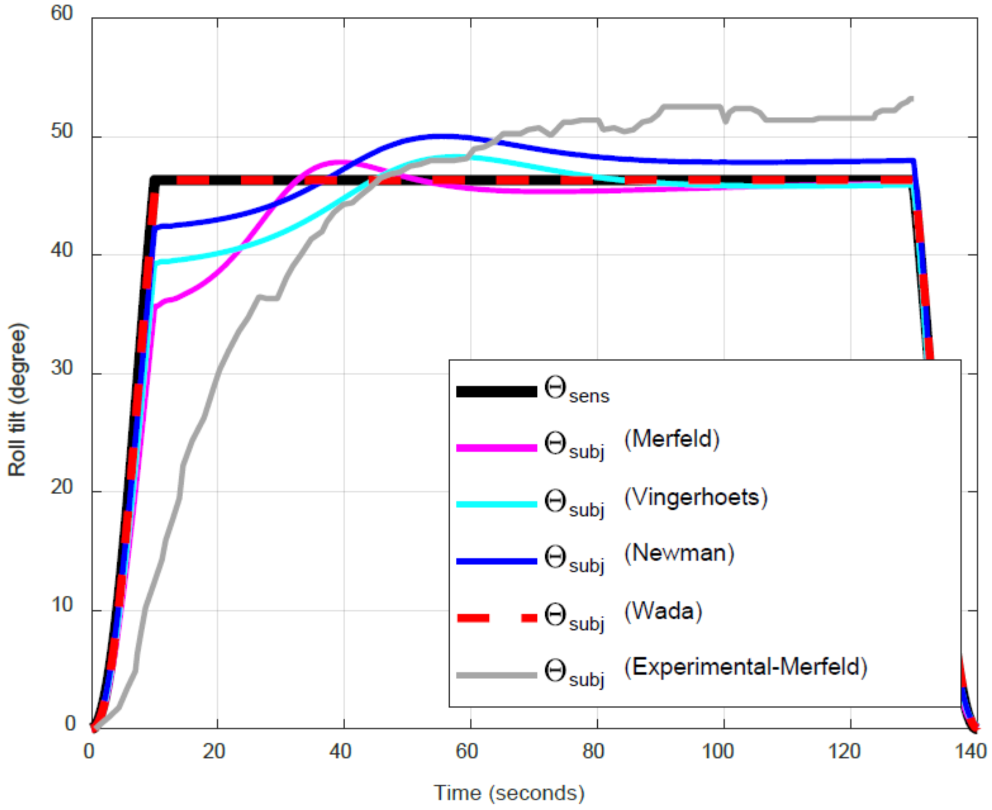

Conclusions and Future Work

- Different human perception models were implemented and evaluated under test conditions.
- The simulation results show that the implemented human perception models are able to predict the human adult range of sensation measured by experimental tests.
- Human perception models can also be tuned to fit with different experimental results of human perception.
- Accurate human perception modelling could improve the prediction of conflict signal estimation.
- Integrating accurate human perception models in motion sickness models can improve their capability to predict motion sickness feelings.
- For future studies, there is still a need to further investigate the integration of human perception models, which includes visual and somatosensory input, as well as improve the nonlinear function part that predicts the feeling of motion sickness.

ilhan.yunus@volvocars.com